

# Stability Functions for Momentum, Heat and Water Vapour and the Vertical Transport of TKE and Pressure Fluctuations Estimated from Measured Vertical Profiles of Wind Speed, Temperature and Humidity\*

by G. KRAMM<sup>1</sup>, F. HERBERT<sup>2</sup>, K. BERNHARDT<sup>3</sup>, H. MÜLLER<sup>1</sup>, P. WERLE<sup>1</sup>,  
T. FOKEN<sup>4</sup>, and S. H. RICHTER<sup>4</sup>

<sup>1</sup>Fraunhofer-Institut für Atmosphärische Umweltforschung (IFU),  
82467 Garmisch-Partenkirchen, Germany

<sup>2</sup>Institut für Meteorologie und Geophysik, Johann Wolfgang Goethe-Universität,  
Postfach 111932,60054 Frankfurt am Main, Germany

<sup>3</sup>Leibniz-Sozietät e.V., Postfach 34,12563 Berlin, Germany

<sup>4</sup>Deutscher Wetterdienst, Meteorologisches Observatorium Lindenberg,  
Dezernat Landoberflächenprozesse und Grenzschicht, 15864 Lindenberg, Germany

(Manuscript received September 5,1995; accepted March 12,1996)

## Abstract

Vertical wind speed, temperature and humidity profile data from three known atmospheric field campaigns are used to determine the surface layer similarity functions for the transport of momentum and heat as well as TKE (turbulent kinetic energy) and pressure fluctuations. The basic principles on which we carry out this determination are a simplified TKE-budget equation obeying Monin-Obukhov similarity laws and a one-and-a-half-order closure concept. Least squares techniques are utilised for the calculations. The numerical analysis provides all important internal and external surface layer parameters like the friction velocity,  $u_*$ , the temperature and humidity scales,  $\theta_*$  and  $q_*$ , the roughness length,  $z_0$ , the zero-plane displacement,  $d$ , as well as the temperature and humidity values  $\theta_r$  and  $q_r$  at the height  $z_r = z_0 + d$ . With these data we can determine the individual  $\gamma$ -coefficients in the empirical Businger-Dyer and O'KEYPS relations. This is the main interest of this study. It is found that the computed empirical coefficients appreciably depend on the thermal stratification in the atmospheric surface layer. These estimates document that the  $\gamma$ 's apparently vary so considerable within a stability regime that the usually adopted constant coefficients were not suitable in these cases. Moreover, one is led to the further important result that the parameters  $z_0$  and  $d$  found here, considerably differ from those values obtained with the conventional  $\gamma$ -coefficients suggested in the literature.

## 1 Introduction

On the basis of profile functions Paulson (1970) has shown that the knowledge of the mean values of wind speed,  $U$ , potential temperature,  $\theta$ , and specific humidity,  $q$ , at two heights  $z_i$  and  $z_{i+1}$  within the atmospheric surface layer is sufficient to

estimate the height-invariant eddy fluxes of momentum, sensible heat and water vapour as well as scaling parameters such as the friction velocity,  $u_*$ , the characteristic heat flux temperature,  $\theta_*$ , and the characteristic water vapour flux humidity,  $q_*$ . Practical insight reveals that some more, external parameters enter the problem, especially the zero-plane displacement,  $d$ , the roughness length,  $z_0$ , as well as the lower boundary level  $z_r = z_0 + d$  at which the values of potential temperature,  $\theta_r = \theta(z_r)$ , and the specific humidity,  $q_r = q(z_r)$ , must be given

\* Dedicated to Dr. Günter Skeib on the occasion of his 75<sup>th</sup> birthday.

If furthermore we assume as significant approaches in order to analyse the non-dimensional similarity functions of wind shear,  $\Phi_m(\zeta)$ , temperature and humidity gradients,  $\Phi_{h,q}(\zeta)$ , such prominent relations as the O'KEYPS equation<sup>1</sup>,

$$\Phi_m^4(\zeta) - \gamma_1 \zeta \Phi_m^3(\zeta) = 1 \quad \text{for } \zeta < 0 \text{ (unstable)} \quad (1)$$

and the specific Businger-Dyer-type expressions (Businger, 1966; Dyer and Hicks, 1970; Webb, 1970)

$$\Phi_m(\zeta) = \begin{cases} 1 + \gamma_2 \zeta & \text{for } \zeta > 0 \text{ (stable)} \\ 1 & \text{for } \zeta = 0 \text{ (neutral)} \\ (1 - \gamma_3 \zeta)^{-1/4} & \text{for } \zeta < 0 \text{ (unstable)} \end{cases} \quad (2)$$

as well as

$$\Phi_h(\zeta) = \begin{cases} \Phi_m(\zeta) & \text{for } \zeta > 0 \\ 1 & \text{for } \zeta = 0 \\ \Phi_m^2(\zeta) & \text{for } \zeta < 0 \end{cases}, \quad (3)$$

$$\Phi_q(\zeta) = \Phi_h(\zeta),$$

we will be led to a set of coefficients  $\gamma_i$  occurring in these formulas which must be specified for any kind of practical use.

With respect to the reduced vertical distance above ground,  $z - d$ , and the Monin-Obukhov stability length  $L$ , a normalised height coordinate,  $\zeta = (z - d)/L$ , is introduced as the relevant independent variable for all non-dimensional similarity functions, mainly  $\Phi_m(\zeta)$  and  $\Phi_h(\zeta)$ , which are imposed as "universal laws describing the surface (constant flux) layer turbulence (see also Bernhardt, 1995).

Special similarity conditions as given in Eqs. (1) to (3) mediate simple connections of the stability profiles belonging to the turbulent heat, water vapour and momentum transfer. The general consensus is that the Dyer-Hicks identity (Dyer and Hicks 1970) for stable stratification ( $\zeta > 0$ ) and Pandolfo's (1996) formula for unstable stratification ( $\zeta < 0$ ); expressing a peculiar turbulent conformity of different quantities (see Eq. (3)) provide a reasonable representation of many experimental data and a useful tool in the practical analysis of surface layers. Pandolfo's relation implies Richardson number  $Ri = \zeta$ . However, as Dyer and Bradley (1982) and Webb (1982) have pointed out, small deviations from that condition may occur.

In the literature over more than two decades (e.g., Lumley and Panofsky, 1964; Dyer and Hicks, 1970; Webb, 1970; Dyer, 1974; Yaglom, 1977; Panofsky

and Dutton, 1984; Högström, 1988) the  $\gamma$ -coefficients are mostly defined as empirical constants, even though the results from a number of serious field experiments show a considerable scatter (see, e.g., Tabs. VI and VII in Högström, 1988) which cannot exclusively be explained by experimental deficiencies. Indeed, with the assumption that the vertical transport of TKE (turbulent kinetic energy) is only to omit in stable air, but plays an important role under lapse conditions, Fortak (1969a, b) as well as Herbert and Panhans (1979) and Panhans and Herbert (1979) concluded that the coefficients  $\gamma_1$  and  $\gamma_3$  are related to the TKE-transport and, therefore, should be significant functions of  $\zeta$ . In keeping with these arguments of the variation of the  $\gamma$ -coefficients and utilising vertical profile data in conjunction with a specific evaluation scheme and an elementary closure hypothesis we will numerically calculate the  $\gamma_i$  as well as estimate their dependence on the thermal stability of surface layer air.

For the analyses we employ a nonlinear computation method. It is based on the strict application of the budget equation of TKE as well as the assumption of the validity of similarity-stability laws. Especially, Eqs. (2) and (3) are used to describe the physical link of heat/matter and momentum transfer.

On account of the role of the TKE-budget equation it is necessary that a closer definition of one of the Monin-Obukhov stability functions is prescribed. Away from the (not so simple) closures discussed and recommended by Fortak (1969a) as well as Herbert and Panhans (1979) and Panhans and Herbert (1979) in the context of surface layer energetics, a most simple and effective criterion is the adoption of Prandtl's neutral mixing length approach. We have chosen this restriction of the more complete concept in view of the very practical purpose of this study and, all the more, since similarity hypotheses have their principal limitations. The numerical analyses are performed with one-and-a-half-order closure principles and least squares techniques. With the input data, consisting of vertical profile measurements of wind speed temperature and humidity, the calculation procedure yields simultaneously the quantities  $\gamma_3$ ,  $z_0$ ,  $d$ ,  $\theta_r(z_r)$  and  $q_r(z_r)$ , the eddy fluxes of momentum, heat and water vapour as well as the vertical transport of TKE and pressure fluctuations. All measured data employed in this study are taken from the Great Plains Turbulence Project (Lettau and Davidson, 1957), the GREIVI 1974 Experiment (Beyer and Roth, 1976), and the LOVENOX Field Experiment of the EUROTRAC subproject BIATEX (Duyzer et al., 1990).

<sup>1</sup> O'KEYPS stands for the initials of various authors who proposed this formula (see Obukhov, 1946; Kazansky and Monin, 1956; Ellison, 1957; Yamamoto, 1959; Panofsky, 1961; Sellers, 1962).

## 2 The TKE Background Concept

In order to introduce an appropriate expression for the local similarity function of wind shear or momentum flux the most convenient conceptional way is to derive it from the budget equation of TKE for steady-state and horizontally homogeneous conditions. Such a TKE-equation reads, using non-dimensional expressions, as follows:

$$0 = -\frac{\Lambda}{\rho u_*^3} \frac{\partial}{\partial z} (E + W) + \frac{\Lambda}{u_*} \left| \frac{\partial \langle \mathbf{v}_H \rangle}{\partial z} \right| + \frac{\Lambda}{\rho u_*^3 c_p \Theta_m} (H + 0.61 c_p \Theta_m Q) - \frac{\Lambda}{\rho u_*^3} \varepsilon. \quad (4)$$

Physically, this reduced TKE-equation (4) establishes, owing to the involved restrictions, a quite elementary balance condition. It consists of the four main effects contributing to the rate of change of TKE which, denoted in the order of the r.h.s. terms of Eq. (4) are the vertical transport of TKE and pressure fluctuations, the production of TKE by kinematic transformation of the mean motion, the thermal gain (unstable air) or loss (stable air) of TKE owing to buoyancy forces, and finally, the dissipation of TKE into the reservoir of heat.

All quantities in Eq. (4) have been used in their conventional notations; so, a characteristic length scale is denoted by  $\Lambda$ , the horizontal wind vector by  $\mathbf{v}_H = (u, v)$  consisting of its  $u, v$ -components, the air density by  $\rho$ , the acceleration of gravity by  $g$ , the specific heat at constant pressure by  $c_p$ , the representative potential temperature for the layer under study by  $\theta_m$ , the dissipation rate by  $\varepsilon$ , the turbulent flux of TKE by  $E = \langle \rho w' e \rangle$  in which  $e = 1/2 (u'^2 + v'^2 + w'^2)$ , the turbulent flux resulting from pressure ( $p$ ) and vertical wind velocity ( $w$ ) fluctuations by  $W = \langle \rho w' p \rangle / \rho$ , the sensible heat flux<sup>2</sup> by  $H = c_p \langle \rho w' \theta \rangle$  as well as the water vapour flux by  $Q = \langle \rho w' q \rangle$ . It is particularly to note that a term in brackets, such as  $E = \langle \rho w' e \rangle$ , symbolises a density-weighted average, and a double prime the departure from that average.

In boundary layer physics Eq. (4) is a very important equation, but, unfortunately, it does not provide a direct means to establish a closed condition for Monin-Obukhov similarity functions because it

still contains several open (unspecified) quantities. In order for the TKE-equation to be obtainable in a similarity function we eliminate  $\varepsilon$  in the dissipation term by means of  $\varepsilon = \rho K_m^3 \Lambda^{-4}$ , a condition often referred to as the von Weizsacker-Heisenberg relation that closely agrees with the Kolmogorov-Prandtl relation,  $K_m = c_m \langle e \rangle^{1/2} \Lambda$  ( $c_m$  being a constant). Then we obtain the TKE-equation

$$0 = -\frac{\Lambda}{\rho u_*^3} \frac{\partial}{\partial z} (E + W) + \frac{\Lambda}{u_*} \left| \frac{\partial \langle \mathbf{v}_H \rangle}{\partial z} \right| + \frac{\Lambda}{\rho u_*^3 c_p \Theta_m} (H + 0.61 c_p \Theta_m Q) - \left\{ \frac{\Lambda}{u_*} \left| \frac{\partial \langle \mathbf{v}_H \rangle}{\partial z} \right| \right\}^{-3}. \quad (5)$$

in which now the length scale  $\Lambda$  is quite obviously the key quantity. Hence, a useful closure condition for  $\Lambda$  should be found so that the differential equation (5) can be converted to an algebraic relationship for Monin-Obukhov-type similarity functions. In believing Stull (1988) and Garratt (1992) the choice of an appropriate length scale might be rather arbitrary. For the problem at hand Fortak (1969a) as well as Herbert and Panhans (1979) postulated the mixing length expression  $\Lambda = \kappa (z-d) \Phi_\Lambda(\zeta)$  with that formula they introduced via  $\Phi_\Lambda(\zeta)$  a further dimensionless stability function for improving the treatment of the length scale in dependence on non-neutral conditions. The latter two authors also examined different expressions for  $\Phi_\Lambda(\zeta)$  and found that its definition at the cost of an analytical hypothesis for the TKE-transport term leads to the most satisfactory agreement with the observational data in Wyngaard and Coté (1971). With that concept one obtains a reasonable determination of the universal profiles of the energy rates in the surface layer as well as an extended representation of the eddy diffusivity for momentum.

The simplest possible case of interest, however, is a Prandtl-type mixing length for neutral stratification,  $\Lambda = \kappa (z-d)$ . The omission of non-neutral effects in  $\Phi_\Lambda(\zeta)$  supposes the argument that buoyancy and mean wind shear may generate turbulence in which the deviation of  $\Phi_\Lambda(\zeta)$  from unity is too small to contribute significantly to the energy dissipation. This concept is usually employed in one-and-a-half-order closure schemes (e.g., Stull, 1988; Garratt, 1992), and also with respect to our concern such a Prandtl-type approach seems us as a sufficient empirical closure condition for  $\Lambda$  in Eq. (5). Hence,

<sup>2</sup> If the definition  $H = \pi c_p \langle \rho w' \theta \rangle$  with  $\pi = T/\theta$  is used for the sensible heat flux then the potential temperature  $\theta_m$  in Eq. (4) must be replaced by the absolute temperature,  $T_m$ .

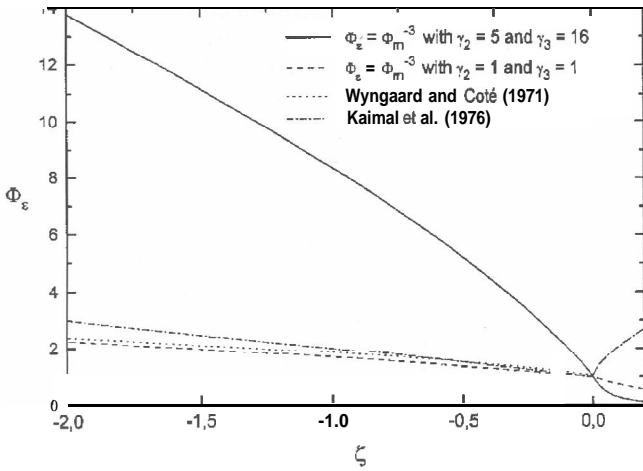


**Figure 1** Comparison of different parameterization approaches for the normalized dissipation  $\Phi_\epsilon(\zeta)$ .

we are led to write this equation in terms of Monin-Obukhov similarity expressions as follows:

$$0 = -\Phi_d(\zeta) + \Phi_m(\zeta) - \zeta - \Phi_\epsilon(5) \quad (6)$$

with  $\Phi_\epsilon(\zeta) = \Phi_m^{-3}(\zeta)$ .

In Eq. (6) the stability functions  $\Phi_d(\zeta)$  and  $\Phi_\epsilon(\zeta)$  represent the dimensionless divergence term and the dimensionless dissipation term, respectively. With a simple reorganisation one easily obtains for Eq. (6) the structure

$$\Phi_m^4(\zeta) - \left( \frac{\Phi_d(\zeta)}{\zeta} + 1 \right) \zeta \Phi_m^3(\zeta) = 1. \quad (7)$$

Equation (7) can be comprised as an extended O'KEYPS equation or, likewise, using the equivalent formulation

$$\Phi_m(\zeta) = \left( 1 - \frac{\frac{\Phi_d(\zeta)}{\zeta} + 1}{\Phi_m(\zeta)} \zeta \right)^{-1/4} \quad (8)$$

as an extended Businger-Dyer expression. But unlike that, which holds only for lapse conditions, Eq. (8) should be relevant in both regimes of unstable and stable stratification.

In the completer physical picture guided by Eqs. (7) or (8) the two coefficients  $\gamma_1$  and  $\gamma_3$  in the conventional O'KEYPS as well as Businger-Dyer relations (1) and (2) are now unveiled as  $\zeta$ -dependent quantities,

$$\gamma_1 = \frac{\Phi_d(\zeta)}{\zeta} + 1 \quad \text{and} \quad \gamma_3 = \frac{\gamma_1}{\Phi_m(5)}. \quad (9)$$

These conditions (9) indicate that, in considering the TKE-budget, neither  $\gamma_1$  nor  $\gamma_3$  can generally be

supposed as invariants of the normalised stability height  $\zeta$ . In consequence, deviations from the conventional values for  $\gamma_1$  and  $\gamma_3$  that will occur in practical cases, should be comprehended as natural. The analysed profiles of the normalised dissipation function  $\Phi_\epsilon(\zeta)$  in Figure 1 may show a qualitative document of this hypothesised  $\gamma$ -behaviour. The departure of the "theoretical"  $\Phi_\epsilon$ -curves (computed with  $\Phi_\epsilon(\zeta) = \Phi_m^{-3}(\zeta)$  owing to Eq. (6) and given  $\gamma$ -values) and the "experimental" curves (determined by Wyngaard and Coté, 1971 as well as Kaimal et al., 1972,1976, by means of observational material) is found to be strongly dependent on the given values for  $\gamma_2$  and  $\gamma_3$  in the  $\Phi_m(\zeta)$ -expression of Eq. (2).

Since Eq. (9) in the equivalent writing

$$\left. \begin{aligned} \Phi_d(5) &= (Y_1 - I) \zeta \\ &= (\gamma_3 \Phi_m(\zeta) - 1) \zeta \end{aligned} \right\} \quad (10)$$

will here be used to determine the similarity function  $\Phi_d(\zeta)$ , one should not let disregarded that the coupled effect of vertical transport of turbulent TKE and pressure fluctuations is manifested in  $\Phi_d(\zeta)$ . If, for example,  $\gamma_1$  is set constant, then, according to Eq. (10),  $\partial(E+W)/\partial z$  would be proportional to the sensible heat flux, as already discussed by Fortak (1969b). Different from that, however, Wyngaard and Coté (1971) have found on empirical basis that only for  $\partial E/\partial z$  a linear law like that seems to be valid. Concerning the pressure fluctuation term one may interpret these authors that they have such effects, in contrast to an approach (5), well associated with a hypothetical, nonlinear imbalance function of  $\zeta$  in their TKE-budget equation.

### 3 The Applied Numerical Schemes

#### 3.1 Profile Functions

With respect to a given  $\zeta_i$  (belonging to height  $z_i$ ) the vertical profile functions for the wind velocity,  $U_i$  the potential temperature,  $\theta_i$ , and specific humidity,  $q_i$ , can be expressed as follows

$$U_i(z_0, d, \gamma_k) = \frac{u_*}{k} \left( \ln \frac{z_i - d}{z_0} - \Psi_m(\zeta_i, \zeta_r) \right), \quad (11)$$

$$\left\{ \begin{aligned} \theta_i(\theta_r) \\ q_i(q_r) \end{aligned} \right\} = \left\{ \begin{aligned} \Theta_r \\ q_r \end{aligned} \right\} + \frac{1}{k} \left\{ \begin{aligned} \Theta_* \\ q_* \end{aligned} \right\} \left( \ln \frac{z_i - d}{z_0} - \Psi_h(\zeta_i, \zeta_r) \right). \quad (12)$$

In the last two equations the terms  $\Psi_m(\zeta_r, \zeta_i)$  and  $\Psi_h(\zeta_r, \zeta_i)$  represent the integral momentum and heat similarity functions for an interval  $[\zeta_r, \zeta_i]$  within the surface layer:

$$\Psi_{m,h}(\zeta_i, \zeta_r) = \int_{\zeta_r}^{\zeta_i} \frac{1 - \Phi_{m,h}(\zeta)}{\zeta} d\zeta. \tag{13}$$

Supposing for forced-convective and stable regimes the Businger-Dyer form of  $\Phi_m(\zeta)$  and  $\Phi_h(\zeta)$  with constant y-coefficients, the integrals in Eq. (13) can be solved analogous to Paulson's (1970) derivation. One obtains for  $\Psi_m(\zeta_r, \zeta_i)$  and  $\Psi_h(\zeta_r, \zeta_i)$  the explicit relations (cf. Kramm and Herbert, 1984; Kramm, 1989)

$$\Psi_m(\zeta_i, \zeta_r) = \begin{cases} -\gamma_2(\zeta_i - \zeta_r) & \text{for } L > 0 \\ 0 & \text{for } L \rightarrow \infty \\ 2 \ln \frac{1 + y_i}{1 + y_r} + \ln \frac{1 + y_i^2}{1 + y_r^2} & \text{for } L < 0, \end{cases} \tag{14}$$

$$- 2 \arctan \frac{y_i - y_r}{1 + y_i y_r} \text{ for } L < 0,$$

$$\Psi_m(\zeta_i, \zeta_r) = \begin{cases} \Psi_m(\zeta_i, \zeta_r) & \text{for } L > 0 \\ 0 & \text{for } L \rightarrow \infty \\ 2 \ln \frac{1 + y_i^2}{1 + y_r^2} & \text{for } L < 0, \end{cases} \tag{15}$$

wherein  $y_i = (1 - \gamma_3 \zeta_{r,i})^{1/4}$  are the reciprocal expressions of the unstable dimensionless wind gradients (see Eq. (2)) at the two heights  $z_r$  and  $z_i$ . Direct calculations with Eqs. (14) and (15) suppose the knowledge of the  $L$ -value; when  $\zeta_r$  approaches to zero (ideal lower boundaries) the resulting  $\Psi_{m,h}(\zeta_i)$  completely agree with Paulson's expressions. Note also that a similar analysis holds correspondingly for examinations with the O'KEYPS equation; this, however, is not explicitly treated here.

Following McBean and Elliott (1975) and considering Eqs. (5) and (6), the vertical transport of kinetic energy and pressure fluctuations in the constant flux layer can be estimated from vertical profiles of wind speed, temperature and humidity by

$$\Delta(E + W) = (E + W)|_{z_i} - (E + W)|_{z_r}$$

$$= -\frac{\rho u_*^3}{\kappa} (\Psi_m(\zeta_i, \zeta_r) + \zeta_i - \zeta_r - \Psi_\varepsilon(\zeta_i, \zeta_r)), \tag{16}$$

where  $\Psi_m(\zeta_i, \zeta_r)$  is given by Eq. (14). The integral similarity function for dissipation,  $\Psi_\varepsilon(\zeta_i, \zeta_r)$ , is defined by

$$\Psi_\varepsilon(\zeta_i, \zeta_r) = \int_{\zeta_r}^{\zeta_i} \frac{1 - \Phi_\varepsilon(\zeta)}{\zeta} d\zeta$$

$$= \int_{\zeta_r}^{\zeta_i} \left( \frac{1}{\zeta} - \frac{1}{\zeta \Phi_m^3(\zeta)} \right) d\zeta. \tag{17}$$

The integral in Eq. (17) is solved with the same  $\Phi_m$ -expressions utilised in the preceding integral functions. Hence, it results for inversion conditions ( $L > 0$ ) to

$$\Psi_\varepsilon(\zeta_i, \zeta_r) = \ln \frac{\Phi_{m,i}}{\Phi_{m,r}} + 2 \gamma_2 \left( \frac{\zeta_i}{\Phi_{m,i}} - \frac{\zeta_r}{\Phi_{m,r}} \right)$$

$$- \frac{\gamma_2}{2} \left( \frac{\zeta_i^2}{\Phi_{m,i}^2} - \frac{\zeta_r^2}{\Phi_{m,r}^2} \right), \tag{18}$$

and for lapse conditions ( $L < 0$ ) to

$$\Psi_\varepsilon(\zeta_i, \zeta_r) = -4 \ln \frac{\Phi_{m,i}}{\Phi_{m,r}} - \ln \frac{1 - \Phi_{m,i}^4}{1 - \Phi_{m,r}^4}$$

$$- \frac{4}{3} \left( \frac{1}{\Phi_{m,i}^3} - \frac{1}{\Phi_{m,r}^3} \right)$$

$$- \ln \frac{(\Phi_{m,i} - 1)(\Phi_{m,r} + 1)}{(\Phi_{m,i} + 1)(\Phi_{m,r} - 1)}$$

$$+ 2 \arctan \frac{\Phi_{m,i} - \Phi_{m,r}}{1 + \Phi_{m,i} \Phi_{m,r}} \tag{19}$$

with  $\Phi_{m,i} = \Phi_m(\zeta_i)$  and  $\Phi_{m,r} = \Phi_m(\zeta_r)$ . Let us notice that all profile functions prepared in this subsection contain uniform parameterizations of the dimensionless wind shear; these are Businger-Dyer-type similarity functions. The physical picture behind such conditions is fairly difficult to understand because height-invariant y-factors in conjunction with the fundamental TKE-concept from Sect. 2 would be rather interpretable as extremely hypothetical. Therefore, we will investigate more precisely, using measured profile data from several field campaigns, whether the constant y-coefficients can well be confirmed or whether a remarkable dependence-of these factors on  $\zeta$  must be conjectured.

### 3.2 Least Squares Techniques

Least squares techniques are applied to estimate the empirical quantities  $\gamma_2$  and  $\gamma_3$  as well as the surface

layer parameters mentioned above from vertical profiles of wind speed, temperature and humidity. Using Eqs. (16) to (19) the vertical transport of kinetic energy by turbulence and pressure fluctuations is estimated, too.

In order to obtain the best approximations for  $\gamma_2$ ,  $\gamma_3$ ,  $z_0$  and  $d$  as well as the reference values  $\theta_r$  and  $q_r$ , we minimise the following expressions

$$|\rho(\mathbf{x})|^2 = \sum_{i=1}^N (U_{M,i} - U_i(\mathbf{x}^T))^2 \quad (20)$$

$$|\eta(\chi_r)|^2 = \sum_{i=1}^N (\chi_{M,i} - \chi_i(\chi_r))^2 \quad (21)$$

$N \geq 4$  (number of observation levels).

For technical reasons we introduced in Eq. (20) the "vector"  $\mathbf{x}^T = (z_0, d, y_k)$ ,  $T$  denoting the transpose of  $\mathbf{x}$ , where

$$\gamma_k = \begin{cases} \gamma_2 & \text{for } L > 0 \\ \gamma_3 & \text{for } L < 0, \end{cases} \quad (22)$$

and

$$\chi = \begin{cases} \Theta, & \text{potential temperature} \\ q, & \text{specific humidity.} \end{cases} \quad (23)$$

Here,  $U_{M,i}$  is the wind speed observed at the height  $z_i \geq z_1$  ( $z_1$  is the lowest observation level),  $\Theta_{M,i}$  and  $q_{M,i}$  are the corresponding values of potential temperature and specific humidity, respectively.

Appropriate values for the scaling parameters  $u_*$ ,  $\theta_*$  and  $q_*$  are provided by the arithmetic averages

$$\begin{Bmatrix} u_* \\ \theta_* \\ q_* \end{Bmatrix} = \frac{1}{N-1} \sum_{j=1}^{N-1} \begin{Bmatrix} u_{*,j} \\ \theta_{*,j} \\ q_{*,j} \end{Bmatrix}, \quad (24)$$

where the quantities  $u_{*,j}$ ,  $\theta_{*,j}$ , and  $q_{*,j}$  are calculated from the profile data collected at the adjacent observation levels  $z_i$  and  $dz_{i+1}$  (for details see Kramm, 1989).

From the minimum (linear leastsquares) condition (21) one obtains the optimum reference values  $\theta_r$  and  $q_r$  as follows

$$\begin{Bmatrix} \Theta_r \\ q_r \end{Bmatrix} = \frac{1}{N} \sum_{i=1}^N \begin{Bmatrix} \Theta_{M,i} \\ q_{M,i} \end{Bmatrix} - \frac{1}{\kappa} \begin{Bmatrix} \Theta_* \\ q_* \end{Bmatrix} \sum_{i=1}^N \left( \ln \frac{z_i - d}{z_0} - \Psi_h(\zeta_i, \zeta_r) \right) \quad (25)$$

The nonlinear least squares Eq. (20) can only be solved by a method of successive approximation. This procedure can be derived from the approximation of the nonlinear least squares formula by series of linear least squares equations, i.e., if  $x$  is an approximation for the optimum solution, then the optimum solution

$$\mathbf{x}^* = \mathbf{x} + (Df(\mathbf{x})^T \cdot Df(\mathbf{x}))^{-1} \cdot Df(\mathbf{x})^T \cdot \rho(\mathbf{x}) \quad (26)$$

of the linear least squares expression

$$\min |\rho(\mathbf{x}) - Df(\mathbf{x}) \cdot (\mathbf{x}^* - \mathbf{x})|^2 \quad (27)$$

is, in general, a better approximation of the nonlinear least squares formula than  $\mathbf{x}$  expressed by  $|\rho(\mathbf{x}^*)|^2 < |\rho(\mathbf{x})|^2$  (Stoer, 1972). The quantity  $Df(\mathbf{x})$  is the Jacobian matrix given by

$$Df(\mathbf{x}) = \begin{Bmatrix} \frac{\partial U_1}{\partial z_0} & \frac{\partial U_1}{\partial d} & \frac{\partial U_1}{\partial \gamma_k} \\ \cdot & \cdot & \cdot \\ \frac{\partial U_N}{\partial z_0} & \frac{\partial U_N}{\partial d} & \frac{\partial U_N}{\partial \gamma_k} \end{Bmatrix} \quad (28)$$

and  $Df(\mathbf{x})^T$  is its transpose. The elements of the Jacobian matrix are listed in the Appendix. To start the iteration procedure, the roughness length and the zero-plane-displacement have to fulfil the conditions:  $z_0^{(1)} > 0$  and  $d^{(1)} < z_1$ . The iteration procedure is terminated if, after the  $m^{\text{th}}$  iteration step, the desired degree of accuracy

$$\begin{aligned} |\gamma_k^{(m+1)} - \gamma_k^{(m)}| &< 0.01 \\ |z_0^{(m+1)} - z_0^{(m)}| &< 0.0001 \text{ m} \\ |d^{(m+1)} - d^{(m)}| &< 0.0001 \text{ m} \end{aligned}$$

is achieved.

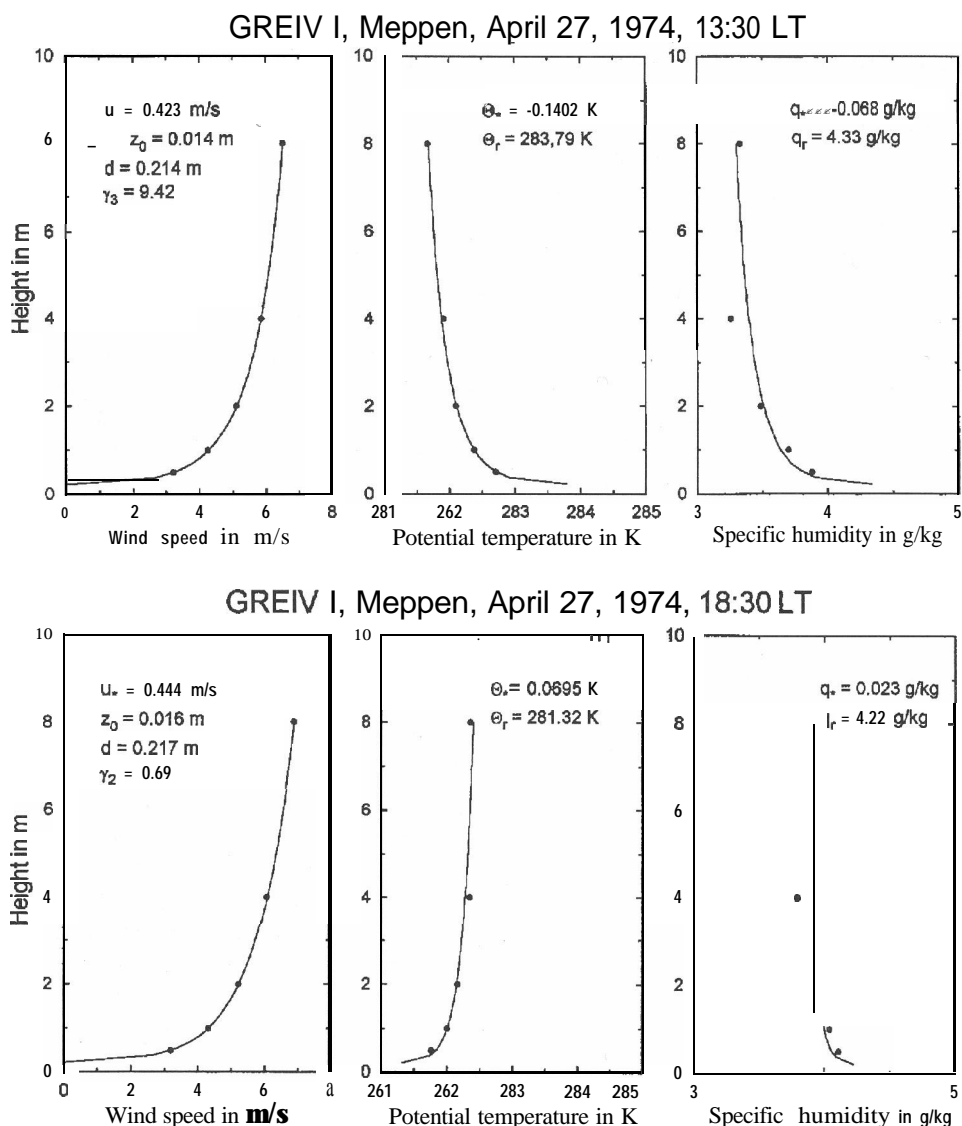


Figure 2 Typical vertical profiles of wind speed, potential temperature and specific humidity calculated for unstable ( $\Theta_* < 0$ ) and stable ( $\Theta_* > 0$ ) conditions. The dots represent the observed values and the solid lines the calculated profiles.

#### 4 Model Tests and Results

Model tests were performed with observational data from the Great Plains Turbulence Project (Lettau and Davidson, 1957), the GREIV I 1974 experiment (Beyer and Roth, 1976), and the LOVENOX field experiment of the EUROTRAC subproject BIA-TEX (Duyzer et al., 1990). The first two data sets were also applied by Kramm (1989) and the latter by Müller et al. (1993) considering  $\gamma_2 = 5$  and  $\gamma_3 = 16$  recommended, for instance, by Panofsky and Dutton (1984).

The Great Plains Turbulence Project was carried out over even terrain near O'Neill, Nebraska, USA, in Summer 1953. The wind (60 min averages), temperature and humidity data (5 min averages) were collected at heights of 0.4, 0.8, 1.6, 3.2 and 6.4 m above ground by the group from the Johns Hopkins University (Lettau and Davidson, 1957).

The GREIV I experiment took place over a flat site, covered with winter barley (about 0.25 m high) and rape (0.50 to 0.75 m high), near Meppen/Emsland in northern Germany in April 1974. Data sets of wind speed, dry- and wet-bulb temperatures (simultaneously measured 30 min averages) were obtained by

groups from the Universities of Kiel (April 20-24, 1974) and Munich (April 24-27, 1974). The observations of the Kiel group were performed at heights of 0.5, 1.26, 3.18 and 8 m and those of the Munich group at heights of 0.5, 1, 2, 4, 8 and 16 m above ground. Note that in the latter case the model calculations were mainly performed with 6 levels, but for some data sets the model converged only when the upper observation level was ignored.

The LOVENOX field was conducted at Halvergate near Great Yarmouth, Norfolk, U.K. This site is a large expanse of drained marshland (grass about 0.10 m, grazed pasture), 1 m above sea level. Fetch extended to over 1 km in most directions and provided excellent micrometeorological conditions, but the disposition of the field equipments restricted the usable fetch to the westerly sector. Wind speed and temperature profiles (20 min averages) were measured by the IFU group at heights of 0.52, 1.00, 1.79, and 3.19 m above ground (Miiller et al., 1993).

If  $t_0 + d > z_l$  or more than 200 iteration steps had been required to determine  $z_0$ ,  $d$ , and  $\gamma_k$ , the profile data sets were generally rejected by the computer program. Such criteria occurred for profile data collected under very stable conditions with low wind velocities and temperature inversions or in the transition phase between lapse and inversion conditions, when stationarity as required by the constant flux concept is not to be expected (Stearns, 1970; Kramm, 1989).

An assessment of the accuracy of this iterating procedure may be performed using the badness of fit (Panofsky and Brier, 1968)

$$\sigma_\chi = \left\{ \frac{1}{N} \sum_{i=1}^N (\chi_{M,i} - \chi_{C,i})^2 \right\}^{1/2}, \quad (29)$$

where  $\chi$  stands for  $U$ ,  $\Theta$ , or  $q$ . Small values of  $\sigma_U$ ,  $\sigma_\Theta$ , and  $\sigma_q$  indicate an excellent matching between the observed and the calculated vertical profiles.

Typical results provided by least squares fitting for different thermal stratification regimes are shown in Figure 2. As illustrated in that figure, the calculated vertical profiles perfectly match the measured profile values which is reflected also in the badness of fit given by  $\sigma_U = 1.1$  cm/s,  $\sigma_\Theta = 0.055$  K, and  $\sigma_q = 0.069$  g/kg for  $\gamma_2 = 0.69$  (inversion conditions), and  $\sigma_U = 0.55$  cm/s,  $\sigma_\Theta = 0.016$  K, and  $\sigma_q = 0.084$  g/kg for  $\gamma_3 = 9.42$  (lapse conditions). Compared with these results, the recommended values  $\gamma_2 = 5$  and  $\gamma_3 = 16$  lead to the slightly larger values of  $\sigma_U = 2.4$  cm/s,  $\sigma_\Theta = 0.056$  K, and  $\sigma_q = 0.070$  g/kg for inversion conditions, and  $\sigma_U = 0.77$  cm/s,

$\sigma_\Theta = 0.021$  K, and  $\sigma_q = 0.085$  g/kg for lapse conditions, respectively.

As especially elucidated by the complete results for the O'Neill data listed in Table 1, different values of  $\gamma_2$  and  $\gamma_3$  can produce very small values of  $\sigma_U$ ,  $\sigma_\Theta$ , and  $\sigma_q$  which hardly differ from each other. Thus, even though small values for the badness of fit are necessary to assure an excellent profile matching, small values alone are insufficient, in general, to decide whether this matching is physically relevant or not. A decision can only be performed if, in addition, physical principles like the budget equation for TKE are considered. The values of  $\gamma_2$  and  $\gamma_3$ , for instance, are usually derived from concurrent measurements of eddy fluxes and vertical profiles where the required gradients of the mean quantities (wind speed, temperature and humidity) are determined by differentiating second-order polynomials in  $\ln(z - d)$  fitted to those mean quantities near the level in question (e.g., Businger et al., 1971; Högl-Strom, 1988). Whereas matching functions which are based, for instance, on TKE-principles (see Eqs. (7) and (8)) lead to other gradients and, as shown here, to other values for  $\gamma_2$  and  $\gamma_3$ .

As also shown in Table 1, especially the results of  $z_0$  and  $d$  derived with the recommended values of  $\gamma_2$  and  $\gamma_3$  considerably differ from those simultaneously provided by our numerical method. Since in most cases the differences in the calculated eddy fluxes are smaller than the precision with which eddy fluxes can directly be measured, the latter cannot simply be used to verify model estimates.

The results obtained from the three experiments are illustrated in Figures 3 to 5 for inversion condition and 6 to 8 for lapse condition, respectively. Figure 3 shows  $\gamma_2$  as a function of  $\zeta^* = z^*/L$  where  $z^*$  is taken as  $z^* = (z_1 z_N)^{1/2}$  to cover the turbulent surface layer under study. Even though the scatter is large, there exists a relationship between  $\gamma_2$  and  $\zeta^*$  indicating that the divergence term is not always negligible. Considering 134 data sets, a mean value of  $\gamma_2$  were  $4.9 \pm 4.7$ . The local stability functions  $\Phi_m(\zeta^*)$ ,  $\Phi_\varepsilon(\zeta^*)$ , and  $\Phi_d(\zeta^*)$  are illustrated in Figure 4 where the respective solid lines, only introduced here to guide the reader's eyes, were derived with that mean value of  $\gamma_2 = 4.9$ . These results substantiate also large scatter especially for  $\Phi_\varepsilon(\zeta^*)$  and  $\Phi_d(\zeta^*)$ . As expected (see Figure 1),  $\Phi_\varepsilon(\zeta^*)$  amounts to smaller values than those obtained from field experiments (Wyngaard and Coté 1971; Kaimal et al., 1976) and, in contrast to those field experiments, decreases with increasing  $\zeta^*$ . Since  $\Phi_d(\zeta^*)$  is related to  $\Phi_\varepsilon(\zeta^*)$  via Eq. (6) larger

**Table 1** Calculated values of the surface layer parameters  $z_0$ ,  $d$ ,  $u_*$ ,  $\theta_*$  and  $q_*$  as well as  $\sigma_U$ ,  $\sigma_\theta$ , and  $\sigma_q$  for the optimized and the recommended values of  $\gamma_2$  and  $\gamma_3$  (from Kramm, 1995). The results are based on the data sets of the Great Plains Turbulence Project (see Lettau and Davidson, 1957).

Julian day	Local time	$z_0$ (cm)	$d$ (cm)	$u_*$ (cm/s)	$\theta_*$ (K)	$q_*$ (g/kg)	$\gamma_2$	$\gamma_3$	$\sigma_U$ (cm/s)	$\sigma_\theta$ (K)	$\sigma_q$ (g/kg)
225	4:35	0.9	-0.5	45.8	0.1359	-0.0192	0.77	-	0.8	0.031	0.020
		0.4	6.6	39.5	0.1161	-0.0163	5.00	-	2.1	0.025	0.019
	6:35	0.3	7.6	35.2	0.0300	-0.0102	11.66	-	0.1	0.013	0.044
		0.5	4.0	37.9	0.0326	-0.0105	5.00	-	1.6	0.013	0.044
	14:35	0.4	5.9	49.9	-0.2164	-0.1896	-	8.53	0.8	0.027	0.038
		0.5	4.0	37.9	-0.2375	-0.0105	-	16.00	2.2	0.032	0.034
16:35	0.5	4.8	44.8	-0.0753	-0.1708	-	25.68	0.8	0.025	0.055	
	0.4	6.6	43.0	-0.0708	-0.1600	-	16.00	1.3	0.026	0.053	
231	6:35	0.2	12.4	19.1	0.0394	-0.0295	14.94	-	1.3	0.053	0.030
		1.5	-4.8	27.9	0.0642	-0.0448	5.00	-	4.1	0.036	0.023
	10:35	0.3	12.4	35.6	-0.2236	-0.1366	-	12.08	3.1	0.057	0.094
		0.4	9.7	37.0	-0.2380	-0.1463	-	16.00	1.2	0.055	0.096
	12:35	0.5	8.0	36.7	-0.4642	-0.1219	-	16.32	0.9	0.173	0.039
		0.5	8.1	36.5	-0.4612	-0.1212	-	16.00	1.5	0.173	0.039
236	12:35	0.4	8.0	62.1	-0.4579	-0.1277	-	12.89	2.2	0.141	0.025
		0.5	7.0	63.6	-0.4789	-0.1334	-	16.00	3.4	0.150	0.027
	16:35	0.5	6.7	60.4	-0.1483	-0.0381	-	20.56	1.2	0.030	0.025
		0.5	7.5	59.4	-0.1446	-0.0370	-	16.00	2.3	0.033	0.025
237	4:35	0.6	6.0	47.7	0.0825	-0.0108	1.27	-	0.3	0.027	0.040
		0.4	9.3	44.6	0.0772	-0.0097	5.00	-	1.2	0.027	0.040
	10:35	0.4	9.9	57.8	-0.2469	-0.0517	-	14.13	0.6	0.058	0.016
		0.4	9.5	58.4	-0.2510	-0.0526	-	16.00	1.2	0.057	0.016
	14:35	0.2	12.3	55.9	-0.2632	-0.0429	-	7.56	2.8	0.018	0.200
		0.3	10.1	59.3	-0.2888	-0.0517	-	16.00	1.9	0.023	0.207
	16:35	0.4	9.3	54.9	-0.1503	-0.0133	-	16.42	1.9	0.029	0.017
		0.4	9.4	54.8	-0.1498	-0.0133	-	16.00	2.1	0.029	0.018
243	4:35	0.5	8.2	36.4	0.0767	-0.0215	1.55	-	0.4	0.018	0.017
		0.3	12.3	33.2	0.0697	-0.0196	5.00	-	1.1	0.016	0.017
	6:35	0.3	13.0	30.6	0.0565	-0.0236	10.98	-	0.5	0.023	0.062
		0.6	6.4	35.5	0.0659	-0.0270	5.00	-	2.0	0.022	0.062
	20:35	0.5	8.4	37.3	0.0148	-0.0117	2.54	-	1.4	0.013	0.210
		0.4	8.7	36.7	0.0146	-0.0134	5.00	-	2.0	0.013	0.210
244	0:35	0.7	2.9	34.4	0.0932	-0.0183	3.74	-	1.5	0.025	0.038
		0.5	5.2	32.8	0.0888	-0.0173	5.00	-	1.5	0.025	0.038
	22:35	0.2	14.4	30.6	0.0809	-0.0035	7.27	-	0.9	0.008	0.014
		0.3	10.6	33.4	0.0882	-0.0038	5.00	-	1.2	0.006	0.014
250	0:35	0.6	7.4	37.4	0.0812	-0.0099	0.90	-	0.8	0.011	0.020
		0.3	12.6	33.2	0.0720	-0.0084	5.00	-	1.6	0.011	0.020
	2:35	1.0	-0.9	36.5	0.1010	0.0087	0.75	-	1.9	0.024	0.059
		0.4	5.8	30.6	0.0840	0.0041	5.00	-	3.5	0.025	0.059
251	12:35	0.3	9.1	55.2	-0.3863	-	-	6.48	4.4	0.102	-
		0.5	5.5	60.0	-0.4455	-	-	16.00	2.8	0.101	-
	14:35	0.3	10.2	52.4	-0.2987	-	-	3.16	3.2	0.075	-
		0.5	5.4	58.5	-0.3555	-	-	16.00	2.9	0.064	-
	16:35	0.5	6.2	53.7	-0.1600	-	-	19.36	0.4	0.028	-
		0.5	6.9	52.9	-0.1559	-	-	16.00	1.8	0.026	-
	18:35	0.6	4.7	39.8	0.0749	-	3.42	-	1.1	0.020	-
		0.4	6.5	38.3	0.0720	-	5.00	-	1.4	0.020	-
251	20:35	0.7	2.5	41.0	0.0759	-	2.94	-	1.0	0.005	-
		0.5	5.1	39.1	0.0723	-	5.00	-	1.9	0.005	-
	22:35	0.5	6.5	29.4	0.0903	-	4.67	-	0.9	0.015	-
		0.4	7.3	28.9	0.0887	-	5.00	-	0.8	0.014	-
0:35	0.4	6.2	29.0	0.0824	-	5.93	-	0.5	0.008	-	
	0.6	3.9	30.4	0.0863	-	5.00	-	0.5	0.009	-	

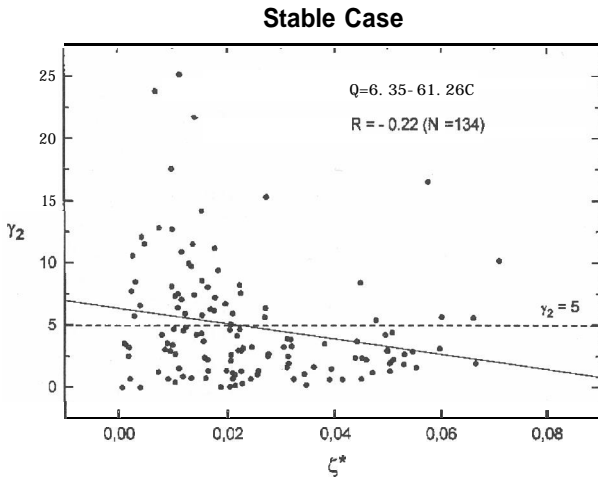


Figure 3 Relationship between  $\gamma_2$  and  $\zeta^*$  in the stable case.

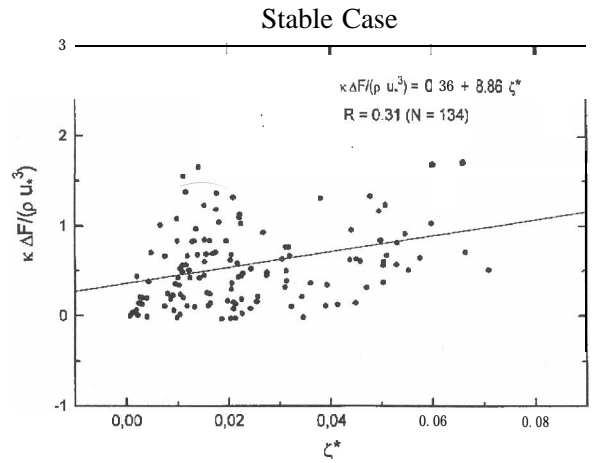


Figure 5 Relationship between  $\kappa \Delta F / (\rho u_*^3)$  and  $\zeta^*$  in the stable case.

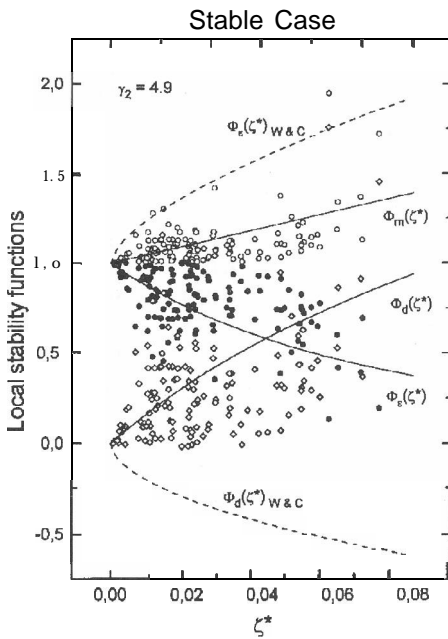


Figure 4  $\Phi_m(\zeta^*)$ ,  $\Phi_e(\zeta^*)$ , and  $\Phi_d(\zeta^*)$  plotted as functions of  $\zeta^*$  for stable stratification. Note that  $\Phi_d(\zeta^*)_{W\&C}$  (according to Wyngaard and Coté, 1971) only contains the transport term.

values of  $\Phi_e(\zeta^*)$  would lead to smaller values of  $\Phi_d(\zeta^*)$ , where also negative values could be possible for increasing  $\zeta^*$  (see Figure 4). As shown in Figure 5, the normalised turbulent transport of both the TKE and the pressure fluctuations characterised by  $\Delta F^* = \kappa \Delta F / (\rho u_*^3)$  (see also Eq. (16)) notably depends on  $\zeta^*$ . However, even though Eq. (16) indicates that  $\Delta F^*$  should approach to zero if  $\zeta^*$  approaches also to zero, this behaviour cannot be described by the simple fitting curve (see Figure 5).

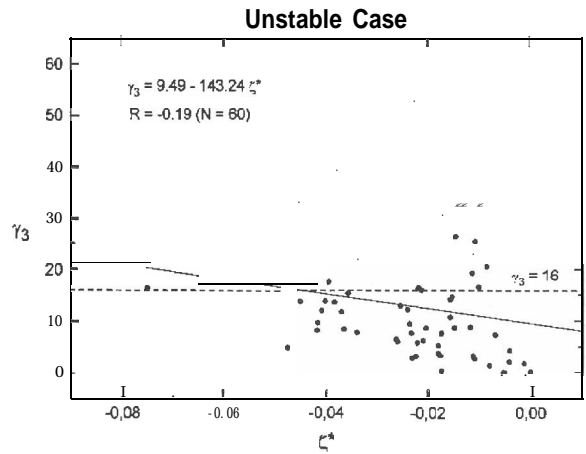


Figure 6 Relationship between  $\gamma_3$  and  $\zeta^*$  in the unstable case.

The quantity  $\gamma_3$  stronger depends on  $\zeta^*$  in the unstable case than  $\gamma_2$  in the stable case (see Figures 3 and 6), but the scatter is large, too. This dependence also substantiates that the divergence term should not be neglected. Considering 60 data sets, a mean value of  $\gamma_3$  were  $12.7 \pm 10.8$ . The stronger dependence of  $\gamma_3$  on  $\zeta^*$  is reflected also in the calculated local stability functions and the normalised turbulent transport of both the TKE and the pressure fluctuations illustrated in Figures 7 and 8,

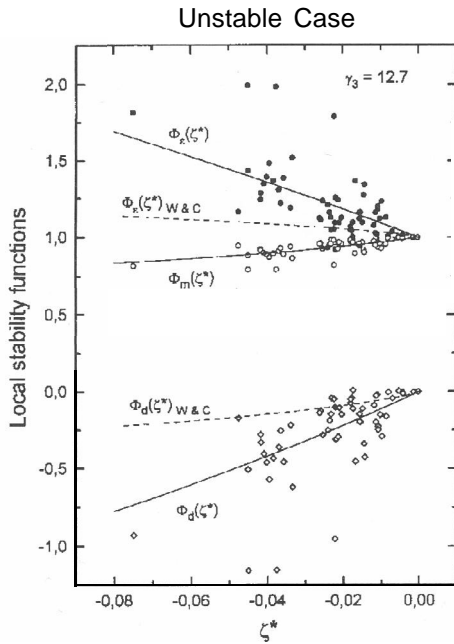


Figure 7 As in Figure 4, but for lapse conditions.

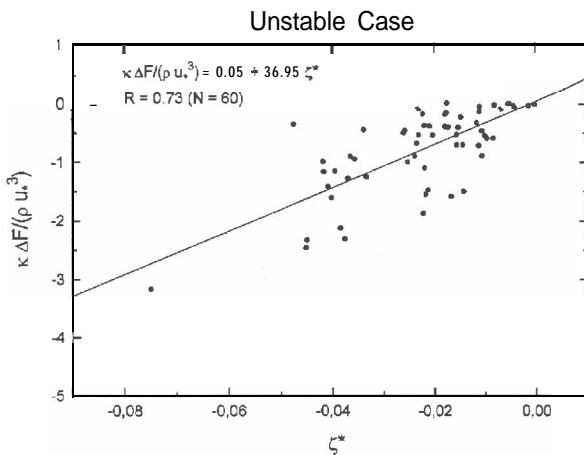


Figure 7 As in Figure 4, but for lapse conditions

respectively. The results for  $\Phi_m(I;^*)$ ,  $\Phi_e(\zeta^*)$ , and  $\Phi_d(\zeta^*)$  shown in Figure 7 evidence a smaller scatter for unstable than for stable stratification, and the respective solid lines (also introduced here to guide the reader's eyes) based on  $\gamma_3 = 12.7$  seem to represent these results well. In contrast to the stable case, the values of  $\Phi_e(\zeta^*)$  exceed those obtained from field experiments (Wyngaard and Coté 1971; Kaimal et al., 1976). This, however, is not surprising because, as shown in Figure 1, those empirical results are represented better by values of  $\gamma_3 \approx 1$ . According to Eq. (6), smaller values of  $\Phi_e(\zeta^*)$  would lead to larger values of  $\Phi_d(\zeta^*)$  (see Figure 7).

As illustrated in Figure 8,  $AF^*$  also stronger depends on  $\zeta^*$  for unstable than for stable stratification. It approaches to zero if  $\zeta^*$  approaches also to zero, in accord with Eq. (16).

### 5 Final Remarks

In approaching a model to investigate the  $\gamma$ -coefficients' postulated dependence on thermal stability which is in studies of the surface layer usually omitted, the stationary turbulent energy budget equation in Monin-Obukhov similarity notation is applied as a basic law. This energy balance is associated with the simple Prandtl condition for the mixing length to obtain extended @versions instead of the O'KEYPS and Businger-Dyer relations.

Consistent with the criteria resulting from these extended @-relations which define explicit  $\gamma(\zeta)$ -functions, our numerical calculations (utilising vertical profile data of wind, temperature and humidity as well as least squares schemes) substantiate the hypothesis that the coefficients  $\gamma_2$  and  $\gamma_3$  (and similarly  $\gamma_1$ ) show appreciable variations in dependence on thermal stratification. Although this behaviour appears to be physically reasonable it must also be seen that we facilitate our treatment by approximating the mixing length via a quasi-neutral approach. Thus, the accuracy of the present model cannot at this point be well estimated since the adopted mixing length is felt to be so simple that it may possibly become unsatisfactory if more serious criteria are required. For instance, this might specifically be true in unstable conditions ( $\zeta < 0$ ) where the production of TKE by the buoyancy activity gradually becomes more important as instability increases. Nevertheless, our numerical results may be regarded as a sufficient qualitative confirmation of the relevance of divergence and export of TKE in the y-expressions of the extended O'KEYPS and Businger-Dyer formulae.

A theory which makes allowance for improvements over the present state must basically consider that a one-and-a-half-order principle such as the TKE-equation (6) and the simultaneous assumption of a conventional scaling length approach (as, e.g., Prandtl's expression) as well as similarity functions of the conventional O'KEYPS or Businger-Dyer type define an overestimated set of equations. In contrast to such models based on conventional scaling length hypotheses, the surface layer energy model of Panhans and Herbert (1979) specifies a theoretical treatment of the loss rates of TKE owing

to vertical export by turbulence as well as owing to viscous dissipation, both being predicted as functions of  $\zeta$ . As a consequence of that concept a scaling length equation as well as a corresponding eddy diffusivity coefficient, both holding for neutral and non-neutral stratification, are obtained.

**Acknowledgements**

We should like to express our thanks to Dr. Nicole Molders from the University of Leipzig, and the anonymous referees for constructive comments.

**Appendix**

The elements of the Jacobian matrix can be approximated by the following expressions:

$$\frac{\partial U_i}{\partial z_o} = \frac{1}{\kappa z_o} \Phi_m(\zeta_r) + \frac{1}{\kappa} \left( \ln \frac{z_i - d}{z_o} - \Psi_m(\zeta_i, \zeta_r) \right) \frac{\partial u_*}{\partial z_o} \tag{A1}$$

$$\frac{\partial U_i}{\partial d} = -\frac{u_*}{\kappa(z_i - d)} \Phi_m(\zeta_i) + \frac{1}{\kappa} \left( \ln \frac{z_i - d}{z_o} - \Psi_m(\zeta_i, \zeta_r) \right) \frac{\partial u_*}{\partial d} \tag{A2}$$

$$\frac{\partial U_i}{\partial \gamma_k} = -\frac{u_*}{\kappa} \frac{\partial}{\partial \gamma_k} \Psi_m(\zeta_i) + \frac{1}{\kappa} \left( \ln \frac{z_i - d}{z_o} - \Psi_m(\zeta_i, \zeta_r) \right) \frac{\partial u_*}{\partial \gamma_k} \tag{A3}$$

where  $\partial \Psi_m(\zeta_i) / \partial \gamma_k$  is given by

$$\frac{\partial}{\partial \gamma_k} \Psi_m(\zeta_i) = \begin{cases} \frac{\Psi_m(\zeta_i)}{\gamma_2} & \text{for } L > 0 \\ -\frac{1}{\gamma_3} (y_i^{-1} - y_o^{-1}) & \text{for } L < 0 \end{cases} \tag{A4}$$

The derivations of  $u_*$  regarding to  $z_o$ ,  $d$ , and  $\gamma_k$ , respectively, can be approximated by

$$\frac{\partial u_*}{\partial z_o} = 0, \tag{A5}$$

$$\frac{\partial u_*}{\partial d} = \frac{1}{N-1} \sum_{j=1}^{N-1} \begin{cases} \frac{1}{z_{i+1}-d} - \frac{1}{z_i-d} u_{*,j} \\ \ln \frac{z_{i+1}-d}{z_i-d} \\ \text{for } L > 0 \\ \frac{y_{i+1}^{-1} - y_i^{-1}}{z_{i+1}-d - z_i-d} u_{*,j} \\ \ln \frac{z_{i+1}-d}{z_i-d} - \Psi_m(\zeta_{i+1}, \zeta_i) \\ \text{for } L < 0, \end{cases} \tag{A6}$$

$$\frac{\partial u_*}{\partial \gamma_k} = \frac{1}{N-1} \sum_{j=1}^{N-1} \begin{cases} \frac{1}{\gamma_2} \left( u_{*,j} - \frac{\kappa(u_{i+1} - u_i)}{\ln \frac{z_{i+1}-d}{z_i-d}} \right) \\ \text{for } L > 0 \\ \frac{y_{i+1}^{-1} - y_i^{-1}}{\ln \frac{z_{i+1}-d}{z_i-d} - \Psi_m(\zeta_{i+1}, \zeta_i)} u_{*,j} \\ \text{for } L < 0. \end{cases} \tag{A7}$$

**References**

**Bernhardt, K., 1995:** Zur Interpretation der Monin-Obuchovschen Lange. Meteorol. Zeitschrift, N.F., 4, 81-82.  
**Beyer, R. and R. Roth, 1976:** GREIV I 1974-Meßdaten. Berichte d. Inst. f. Meteor. u. Klimat. d. TU Hannover 16.  
**Businger, J. A., 1966:** Transfer of momentum and heat in the planetary boundary layer. In: Proceedings of the Symposium on Arctic Heat Budget and Atmospheric Circulation The Rand Corporation, 305-332.  
**Businger, J. A., J. C. Wyngaard, Y. Izumi and E. F. Bradley, 1971:** Flux-profile relationships in the atmospheric surface layer. J. Atmos. Sci. 28,181-189.  
**Duyzer, J. H., D. Fowler, F. X. Meixner, G. Dollard, C. Johansson and M. Gallinger, 1990:** The Halvergate trace gas experiment on surface exchange of oxides of nitrogen: Preliminary results. In: S. Beilke, M. Millan, G. Angeletti (eds.), Field measurements and interpretation of species derived from NO<sub>2</sub>, NH<sub>3</sub>, and VOC emission in Europe. Air pollution research report 25, Commission of the European Communities, Brussels, Belgium, 267-276.  
**Dyer, A. J. and B. B. Hicks, 1970:** Flux-gradient relationships in the constant flux layer. Quart. J. R. Met. Soc. 96, 715-721.  
**Dyer, A. J., 1974:** A review of flux-profile relationships. Boundary-Layer Meteorol. 7, 363-372.  
**Dyer, A. J. and E. F. Bradley, 1982:** An alternative analysis of flux-gradient relationships at the 1976 ITCE. Boundary-Layer Meteorol. 22, 3-19.  
**Ellison, T. H., 1957:** Turbulent transport of heat and momentum from an infinite rough plane. J. Fluid Mech. 2, 456-466.

- Fortak, H.**, 1969a: Berechnung des charakteristischen "Scales" der Turbulenz der bodennahen Grenzschicht aus Windprofilmessungen. Beitr. Phys. Atmos. 42, 245-250.
- Fortak, H.**, 1969b: Zur Energetik der planetarischen Grenzschicht. Annalen der Meteorologie (NF) 4,157-162.
- Garratt, J.R.**, 1992: The atmospheric boundary layer. Cambridge University Press, 316 pp.
- Herbert, F. and W. G. Panhans**, 1979: Theoretical studies of the parameterization of the non-neutral surface boundary layer - Part I: Governing physical concepts. Boundary-Layer Meteorol. 16,155-167.
- Högström, U.**, 1988: Non-dimensional wind and temperature profiles in the atmospheric surface layer: A re-evaluation. Boundary-Layer Meteorol. 42,55-78.
- Kairnal, J. C., J. C. Wyngaard, Y. Izumi and O. R. Coté**, 1972: Spectral characteristics of surface layer turbulence. Quart. J. R. Met. Soc. 98,563-589.
- Kaimal, J. C., J. C. Wyngaard, D. A. Haugen, O. R. Coté, Y. Izumi, S. J. Caughey and C. J. Readings**, 1976: Turbulence structure in the convective boundary layer. J. Atmos. Sci. 33,2152-2169.
- Kazansky, A. B. and A. S. Monin**, 1956: Turbulence in the inversion layer near the surface. Izv. Acad. Nauk. SSSR Ser. Geophys. 1,79-86.
- Kramm, G. and F. Herbert**, 1984: Ein numerisches Modell zur Deposition von Schadstoffen in der bodennahen Luftschicht. In: H. Reuter (Ed.), Probleme der Umwelt- und Medizinmeteorologie im Gebirge, Symposium Rauris/Österreich, September 23-25, 1983. Zentralanstalt f. Meteorologie u. Geodynamik, Wien, Nr. 288,22-38.
- Kramm, G.**, 1989: The estimation of the surface layer parameters from wind velocity, temperature and humidity profiles by least squares methods. Boundary-Layer Meteorol. 48,315-327.
- Kramm, G.**, 1995: Zum Austausch von Ozon und reaktiven Stickstoffverbindungen zwischen Atmosphäre und Biosphäre. Wissenschafts-Verlag Dr. W. Marau, Frankfurt/Main, 268 pp.
- Lettau, H. H. and B. Davidson**, 1957: Exploring the atmosphere's first mile. Vol. 1 and 2, Pergamon Press, New York.
- Lumley, J. L. and H. A. Panofsky**, 1964: The structure of atmospheric turbulence. Interscience Publishers (J. Wiley & Sons), New York/London/Sydney, 239 pp.
- McBean, G. A. and J. A. Elliott**, 1975: The vertical transport of kinetic energy by turbulence and pressure in the boundary layer. J. Atmos. Sci. 32,753-766.
- Müller, H., G. Kramm, F. Meixner, D. Fowler, G. J. Dollard, M. Possanzini**, 1993: Determination of HNO<sub>3</sub> dry deposition by modified Bowen ratio and aerodynamic profile techniques. Tellus 45B, 346-367.
- Obukhov, A. M.**, 1946: Turbulentnost' v temperaturneodnorodnoj atmosphere. Trudy Inst. Teor. Geofiz., AN. SSSR 1, 195-115 (English transl. in: Boundary-Layer Meteorol. 2,1971,7-29).
- Pandolfo, J.**, 1966: Wind and temperature profiles for a constant flux boundary layer in lapse conditions with a variable eddy conductivity to eddy viscosity ratio. J. Atmos. Sci. 23,495-502.
- Panhans, W. G. and F. Herbert**, 1979: Theoretical studies of the parameterization of the non-neutral surface boundary layer - Part II: An improved similarity model. Boundary-Layer Meteorol. 16,169-179.
- Panofsky, H. A.**, 1961: An alternative derivation of the diabatic wind profile. Quart. J. R. Met. Soc. 87,109-110.
- Panofsky, H. A. and G. W. Brier**, 1968: Some applications of statistics to meteorology. Penn State University.
- Panofsky, H. A. and J. A. Dutton**, 1984: Atmospheric turbulence. John Wiley & Sons, New York/Chichester/Brisbane/Toronto/Singapore, 397 pp.
- Paulson, C. A.**, 1970: The mathematical representation of wind speed and temperature profiles in the unstable atmospheric surface layer. J. Appl. Meteor. 9,857-861.
- Sellers, W. D.**, 1962: Simplified derivation of the diabatic wind profile. J. Atmos. Sci. 19,180-181.
- Stearns, C. R.**, 1970: Determining surface roughness and displacement height. Boundary-Layer Meteorol. 1, 102-111.
- Stoer, J.**, 1972: Einführung in die numerische Mathematik I. Springer, Berlin/Heidelberg/New York/Tokyo, 250 pp.
- Stull, R. B.**, 1988: An introduction to boundary layer meteorology. Kluwer Academic Publishers, Dordrecht/Boston/London, 666 pp.
- Webb, E. K.**, 1970: Profile relationships: the log-linear range, and extension to strong stability. Quart. J. R. Met. Soc. 96,67-90.
- Webb, E. K.**, 1982: Profile relationships in the super adiabatic surface layer. Quart. J. R. Met. Soc. 108,661-688.
- Wyngaard, J. C. and O. R. Coté**, 1971: The budget of turbulent kinetic energy and temperature variance in the atmospheric surface layer. J. Atmos. Sci. 28,190-201.
- Yaglom, A. M.**, 1977: Comments on wind and temperature flux-profile relationships. Boundary-Layer Meteorol. 11, 89-102.
- Yamamoto, G.**, 1959: Theory of turbulent transfer in non-neutral conditions. J. Meteor. Soc. Japan